

# 1 **Impacts of anthropogenic water regulation on global** 2 **riverine dissolved organic carbon transport**

3 Yanbin You<sup>1,2</sup>, Zhenghui Xie<sup>1,2\*</sup>, Binghao Jia<sup>1\*</sup>, Yan Wang<sup>3</sup>, Longhuan Wang<sup>1</sup>, Ruichao  
4 Li<sup>1</sup>, Heng Yan<sup>1,2</sup>, Yuhang Tian<sup>1,2</sup>, Si Chen<sup>1,2</sup>

5 <sup>1</sup>State Key Laboratory of Numerical Modeling for Atmospheric Sciences and Geophysical Fluid  
6 Dynamics, Institute of Atmospheric Physics, Chinese Academy of Sciences, Beijing 100029, China

7 <sup>2</sup>College of Earth and Planetary Sciences, University of Chinese Academy of Sciences, Beijing 100049,  
8 China

9 <sup>3</sup>State Key Laboratory of Hydrology-Water Resources and Hydraulic Engineering, Nanjing Hydraulic  
10 Research Institute, Nanjing 210029, China

11 *Correspondence to:* Zhenghui Xie (zxie@lasg.iap.ac.cn), [Binghao Jia \(bhjia@mail.iap.ac.cn\)](mailto:Binghao Jia (bhjia@mail.iap.ac.cn))

12 **Abstract.** Anthropogenic water regulation activities, including reservoir interception, surface water  
13 withdrawal, and groundwater extraction, alter riverine hydrologic processes and affect dissolved organic  
14 carbon (DOC) export from land to rivers and oceans. In this study, schemes describing soil DOC leaching,  
15 riverine DOC transport, and anthropogenic water regulation were developed and incorporated into the  
16 Community Land Model 5.0 (CLM 5.0) and the River Transport Model (RTM). Three simulations by the  
17 developed model were conducted on a global scale from 1981 to 2013 to investigate the impacts of  
18 anthropogenic water regulation on riverine DOC transport. The validation results showed that DOC  
19 exports simulated by the developed model were in good agreement with global river observations. The  
20 simulations showed that DOC transport in most rivers was mainly influenced by reservoir interception  
21 and surface water withdrawal, especially in central North America and eastern China. Four major rivers,  
22 including the Danube, Yangtze, Mississippi, and Ganges Rivers, have experienced reduced riverine DOC  
23 flows due to intense water management, with the largest effect occurring in winter and early spring. In  
24 the Danube and Yangtze River basins, the impact in 2013 was four to five times greater than in 1981,  
25 with a retention efficiency of over 50 %. The Ob River basin was almost unaffected. The total impact of  
26 anthropogenic water regulation reduced global annual riverine DOC exports to the ocean by  
27 approximately  $13.36 \pm 2.45$  Tg C yr<sup>-1</sup>, and this effect increased from 4.83 % to 6.20 % during 1981–  
28 2013, particularly in the Pacific and Atlantic Oceans.

29 **1. Introduction**

30 Rivers are a pipe linking the two major carbon pools of terrestrial and ocean ecosystems and are one of  
31 the key hubs of the global carbon cycle (Cole et al., 2007). According to the [Fifth Assessment Report of](#)  
32 [the Intergovernmental Panel on Climate Change \(IPCC AR5\)](#), terrestrial ecosystems deliver about 1.7 Pg  
33 C per year to rivers through surface and subsurface runoff and about 0.9 Pg C per year to oceans via  
34 rivers. [Approximately 0.21 Pg of this](#) is dissolved organic carbon (DOC) (Ludwig et al., 1996), [which is](#)  
35 equivalent to about 1 % of the global net primary productivity (NPP) of terrestrial ecosystems (Zhang,  
36 2012). Riverine DOC is a [rather highly](#) reactive organic carbon, easily decomposed. [It is](#) a direct source  
37 of carbon for microbial food webs in rivers and oceans, as well as a source of greenhouse gas emissions  
38 from freshwater systems (Li et al., 2019; Tranvik & Jansson, 2002). It deeply affects the biogeochemical  
39 cycles of rivers and offshore ecosystems. Therefore, it is important to clarify the transport characteristics  
40 of riverine DOC for estimating global carbon budgets.

41 In recent years, anthropogenic water management activities, including reservoir interception, surface  
42 water withdrawal, and groundwater extraction, have intensified the degree of interference with natural  
43 processes on the surface of river basins, altered the hydrological and hydraulic processes of rivers, and  
44 affected material circulation and transportation (Zhang, 2012). For example, extraction from  
45 underground aquifers affects hydrological systems, leading to a reduction in subsurface runoff and  
46 eventually to decreased soil [carbon losses](#) (Zeng et al., 2016). [Whereas](#) activities such as irrigation can  
47 lead to increased surface runoff, resulting in increased soil carbon losses (Ren et al., 2016). Artificially  
48 constructed large reservoirs or dams disrupt the carbon cycle balance of the river continuum in its natural  
49 state (Maavara et al., 2017), resulting in retention of DOC and sediment, while lower river velocities and  
50 higher material concentrations lead to increased microbial activity in the water body, thus changing the  
51 nutrient state of the river ecosystem (Liu et al., 2022). However, the impact of these anthropogenic  
52 disturbances on riverine carbon transport has been ignored in estimating the global carbon budget  
53 (Regnier et al., 2013).

54 Based on field surveys involving global riverine DOC transport flux estimation, the United Nations  
55 Environment Programme has constructed a world river discharge database, GEMS-GLORI, that lists 48  
56 attributes of 555 major world rivers (Meybeck, 1982; Meybeck & Ragu, 2012). There are also regional  
57 survey programs, such as the Pan-Arctic River Transport of Nutrients, Organic Matter, and Suspended

删除了: , of which about

删除了: . This

删除了: higher

删除了: is

删除了: ,

删除了: and i

删除了: rivers, reservoirs, and

删除了: DOC

删除了: leaching

删除了: (Zeng et al., 2016),

删除了: w

69 Sediments (PARTNERS, <https://arcticgreatrivers.org/>) and the United States Geological Survey (USGS)  
70 Data Center (<https://waterdata.usgs.gov/nwis>), which provide riverine organic carbon flux data for parts  
71 of large rivers. Field survey studies are directly limited by data availability and completeness and  
72 therefore mostly focus on large rivers in developed regions, making it difficult to cover rivers in other  
73 regions. Moreover, only annual averages are usually available, with no **long-term** time series variation.  
74 Some researchers have started to explore the mechanisms of riverine carbon flux changes using empirical  
75 statistical models, which combine observed data with driving factors including river basin characteristics  
76 (Ludwig et al., 1996), soil carbon and nitrogen ratios (Aitkenhead & McDowell, 2000), land-cover types  
77 (Harrison et al., 2005), and river discharge (Fabre et al., 2020). However, the empirical statistical method  
78 does not consider complex ecological processes within the watershed and cannot describe material  
79 changes in the river network in detail. To identify changes in carbon transport and its driving mechanisms  
80 spatially and explicitly, numerous process-based numerical models are currently used for DOC transport  
81 simulations. Futter et al. (2007) proposed the integrated catchments model for carbon (INCA-C), which  
82 explicitly considers land use, hydrological processes, soil carbon biogeochemical cycles, and surface  
83 water processes. Liao et al. (2019) developed a three-dimensional terrestrial ecosystem model (ECO3D)  
84 considering the influence of lateral water flows. These models simulate regional riverine DOC dynamics  
85 more accurately than earlier models, but their accuracy relies on complex parametric schemes of eco-  
86 hydrological processes and extensive data surveys, so that it is difficult to extend these models to global-  
87 scale simulations. Wu et al. (2014) integrated ecological driving factors and biogeochemical processes  
88 to develop a TRIPLEX-DOC model that predicts DOC metabolism, sorption, desorption, and loss  
89 processes in soils. Li et al. (2019) added a river hydrological process module to construct the TRIPLEX-  
90 HYDRA model and applied it to simulate global riverine DOC fluxes. However, the model did not  
91 consider the impact of human activities on riverine DOC transport. Tian et al. (2015) constructed the  
92 dynamic land ecosystem model (DLEM), a fully distributed model that integrates vegetation dynamics  
93 with processes such as water, carbon, nitrogen, and phosphorus cycling and the effects of human activities  
94 and climate change to simulate DOC flux transport in eastern North American rivers. To better quantify  
95 riverine carbon transport processes at watershed scale, Yao et al. (2021) coupled the scale-adaptive water  
96 transport model (Li et al., 2013) to the DLEM model and applied the result to two mid-Atlantic  
97 watersheds in the United States. Nevertheless, these models failed to consider the effects of

删除了:-

99 anthropogenic water regulation activities. Furthermore, constructing numerical simulation models is a  
100 future development direction of riverine carbon flux estimation; at present, models are still not widely  
101 used to simulate riverine carbon transport (Camino-Serrano et al., 2018).

102 In this study, we incorporated global soil and riverine DOC transport schemes considering  
103 anthropogenic water regulation activities into Community Land Model 5.0 (CLM5.0) and conducted  
104 numerical simulations at global scale (spatial resolution of about 1° for the land processes and 0.5° for  
105 the river systems) during 1981–2013 to explore the impact of anthropogenic water regulation activities  
106 on land-to-ocean riverine DOC transport.

## 107 2. Model Development

### 108 2.1. Model Overview

109 The model was developed based on CLM5.0, which is the land component of the CESM (Community  
110 Earth System Model). CLM is widely used to simulate and study land surface ecohydrological processes,  
111 surface energy exchange processes, and other biogeochemical processes. The latest version of CLM  
112 updates most components of previous versions, explicitly represents land-use and land-cover change,  
113 introduces a revised canopy interception parameterization, and significant improvements in soil layer  
114 resolution, nitrogen cycle, and the snow model. Moreover, CLM5.0 includes two river routing methods:  
115 the Model for Scale Adaptive River Transport (MOSART, Li et al., 2013) and the River Transport Model  
116 (RTM). Because the scale of this study was global, the river transport model still uses linear scheme RTM.

117 However, CLM5.0 lacks an expression of the soil DOC leaching process and the DOC transport and  
118 transformation process in rivers. Therefore, in this paper, schemes for DOC leaching in soils and DOC  
119 transport in rivers will be proposed and incorporated into CLM5.0 to simulate riverine carbon transport.  
120 To investigate the effect of anthropogenic water regulation activities on global riverine DOC transport,  
121 this study used the scheme proposed by Zeng et al. (2016), and coupled it with DOC transport processes.  
122 The model framework is shown in Fig. 1.

删除了:(

删除了:)

删除了: The latest version of CLM updates most components of previous versions, explicitly represents land-use and land-cover change, introduces a revised canopy interception parameterization, and uses the Model for Scale Adaptive River Transport (MOSART, Li et al., 2013) to replace the original River Transport Model (RTM), in addition to significant improvements in soil layer resolution, nitrogen cycle, and the snow model. Because the scale of this study was global, the river transport model still uses linear RTM.

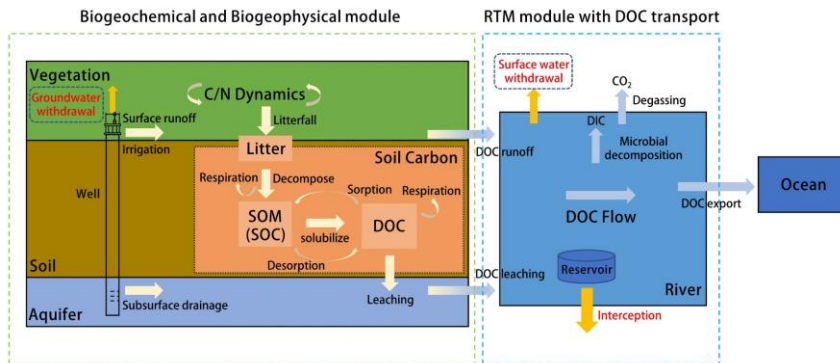


**Figure 1.** Schematic diagram of the land surface model with riverine dissolved organic carbon (DOC) transport and anthropogenic water regulation (C: carbon; N: nitrogen; SOM: soil organic matter; SOC: soil organic carbon; DIC: dissolved inorganic carbon).

134 **2.2. Soil DOC loss to the river**

135 Riverine DOC is mainly derived from organic carbon leaching processes in soil ecosystems in the  
 136 watershed (Gommet et al., 2022; Li et al., 2019). In CLM5.0, only the leaching process of soil mineral  
 137 nitrogen is included, and therefore a DOC production and loss process was introduced in this study. The  
 138 soil biochemistry module in CLM5.0 was constructed based on the Century model (Parton et al., 1988),  
 139 in which the decomposition of fresh litter into soil organic matter is defined as a transformation cascade  
 140 between the coarse woody debris (CWD) pool, the litter pool, and the soil organic matter (SOM) pool.  
 141 The NPP produced by plants eventually enters the soil in the form of litter to constitute the soil carbon  
 142 pool, accompanied by an intervening loss through microbial heterotrophic respiration. Assuming that  
 143 dissolved organic matter (DOM) production is part of the turnover of litter pools and soil organic matter  
 144 pools and is proportional to soil water content, DOC production can be expressed as (Gerber et al., 2010):

$$P_{DOC,u \rightarrow d} = f_{DOM} \theta CF_{u \rightarrow d}, \quad (1)$$

146 where  $P_{DOC,u \rightarrow d}$  ( $\text{g C m}^{-2} \text{s}^{-1}$ ) is the DOC flux from the decomposition process;  $f_{DOM}$  is the fraction  
 147 that enters the soil DOM pool;  $\theta$  ( $\text{m}^3 \text{m}^{-3}$ ) is the soil water content; and  $CF_{u \rightarrow d}$  ( $\text{g C m}^{-2} \text{s}^{-1}$ ) is the  
 148 carbon flux from upstream to downstream carbon pools in the decomposition cascade.

149 Soil organic carbon remaining after plant growth and soil respiration is subject to loss as a dissolved  
 150 component leaching from the soil column. In this study, the DOC<sub>r</sub> runoff is defined as the soil DOC in  
 151 surface runoff, and the DOC leaching is defined as the subsurface losses of DOC in soil water. The  
 152 general equation is written as:

删除了: Riverine DOC is mainly derived from organic carbon leaching processes in soil ecosystems in the watershed

删除了: The

156  
157  
158  
159  
160  
161  
162  
163  
164  
165  
166  
167  
168  
169  
170  
171  
172  
173  
174  
175  
176  
177  
178  
179  
180  
181  
182

$$DOC_{loss} = [DOC]Q_s k_{adsorb} - SR, \quad (2)$$

where  $DOC_{loss}$  ( $\text{g C m}^{-2} \text{ s}^{-1}$ ) denotes the soil DOC runoff or leaching,  $Q_s$  ( $\text{kgH}_2\text{O m}^{-2} \text{ s}^{-1}$ ) denotes the surface runoff or subsurface discharge,  $[DOC]$  ( $\text{g C kgH}_2\text{O}^{-1}$ ) is the DOC concentration in the soil water solution;

$$[DOC] = \frac{NS_{DOC}}{WS_{tot\ soil}}, \quad (3)$$

where  $WS_{tot\ soil}$  ( $\text{kgH}_2\text{O m}^{-2}$ ) is the total mass of soil water content integrated over the soil column and  $NS_{DOC}$  ( $\text{g C m}^{-2}$ ) is the DOC in the soil pool.

Soil DOC readily complexes with metal ions in the soil and forms soil agglomerates, which enable soil DOC to be adsorbed onto soil particles. The DOC adsorption coefficients can be estimated as (Li et al., 2019; Neff & Asner, 2001):

$$k_{adsorb} = \frac{X_i}{X_i + RE}, \quad (4)$$

$$RE = mX_i - b, \quad (5)$$

where  $X_i$  ( $\text{mg g soil}^{-1}$ ) represents the initial DOC concentration,  $RE$  ( $\text{mg g soil}^{-1}$ ) is the amount of DOC desorbed (negative value) or adsorbed (positive value), calculated by the simple initial mass (IM) linear isotherm,  $m$  (dimensionless coefficient) and  $b$  ( $\text{mg g soil}^{-1}$ ) can be considered as measures of potential DOC sorption and desorption by soil.

The soil heterotrophic respiration flux of DOC,  $SR$  ( $\text{g C m}^{-2} \text{ s}^{-1}$ ), is estimated by an empirical function (Janssens and Pilegaard, 2003):

$$SR = R_{10} Q_{s10}^{\frac{T-10}{10}}, \quad (6)$$

where  $T$  ( $^{\circ}\text{C}$ ) is the soil temperature;  $R_{10}$  is the soil heterotrophic respiration flux at a soil temperature of  $10^{\circ}\text{C}$ ;  $Q_{s10}$  is the soil respiration temperature sensitivity.

It is necessary to limit the total DOC runoff/leaching flux at each time step so that it does not exceed the total amount of DOC:

$$DOC_{loss} = \min(DOC_{loss}, \frac{NS_{DOC}}{\Delta t}). \quad (7)$$

### 2.3. Riverine DOC transport

Soil DOC enters the river network system along with surface and subsurface runoff, where it is lost due to processes such as microbial degradation. Therefore, based on the water transport framework, the large-

带格式的: 右侧: 0 厘米, 制表位: 不在 20 字符 + 38 字符  
删除了: Where  
设置了格式: 字体: Times New Roman  
设置了格式: 字体: Times New Roman  
删除了:  
删除了: calculated as

删除了: and

删除了:  $DOC_{leached} = m$

188 scale riverine DOC transport equation can be defined as:

$$189 \quad \frac{dS_{DOC}}{dt} = F_{DOC}^{in} - F_{DOC}^{out} + R_{DOC} + L_{DOC} - k_{doc} * Q_{10}^{\frac{rt-20}{10}} * S_{DOC}, \quad (8)$$

190 where  $S_{DOC}$  (kg C) is DOC storage within the current grid cell;  $R_{DOC}$  (kg C s<sup>-1</sup>) and  $L_{DOC}$  (kg C s<sup>-1</sup>)  
191 represent soil DOC runoff and leaching;  $k_{doc}$  (s<sup>-1</sup>) is the DOC decomposition rate in the river;  $Q_{10}$   
192 (=2.0) denotes the temperature coefficient;  $rt$  (°C) represents the river water temperature, which is  
193 calculated by a large-scale river water temperature model (Liu et al., 2020; van Vliet et al., 2012; Yearsley,  
194 2009);  $F_{DOC}^{in}$  (kg C s<sup>-1</sup>) is the sum of inflows of riverine DOC from neighboring upstream grid cells;  
195 and  $F_{DOC}^{out}$  (kg C s<sup>-1</sup>) is the riverine DOC flux leaving the current grid cell, which is calculated as follows:

$$196 \quad F_{DOC}^{out} = \frac{vS_{DOC}}{d}, \quad (9)$$

197 where  $v$  (m s<sup>-1</sup>) is the effective riverine flow velocity, which is estimated by a simplified Manning's  
198 equation (Oleson et al., 2013);  $d$  is the Euclidean distance between two adjacent grid-cell centers.

#### 199 **2.4. Anthropogenic water regulation**

200 Anthropogenic water regulation includes reservoir interception, surface water withdrawal, and  
201 groundwater extraction and use. Because reservoir interception and surface water withdrawal are closely  
202 related, they are together called surface water regulation. This study coupled the global reservoir  
203 operation scheme (Hanasaki et al., 2006) with RTM using the method of Liu et al. (2019) to represent  
204 the interception effect of reservoirs on runoff and solutes. The method assumed that the inflow from the  
205 reservoir was the outflow from the current grid cell. Released flow from the reservoir was adjusted for  
206 specific uses (flood control, irrigation, etc.), and surface withdrawals were deducted from the released  
207 water (see Sect. S1 in the Supplement).

208 Surface water is extracted directly from natural rivers and reservoirs to meet human water demands  
209 (Wang et al., 2020; Xie et al., 2020; Liu et al., 2019):

$$210 \quad S_{sw}' = S_{sw} - q_{sw} \Delta t, \quad (10)$$

211 where  $S_{sw}'$  (mm) is the surface water storage after extraction;  $S_{sw}$  (mm) is the original surface water  
212 storage;  $q_{sw}$  (mm s<sup>-1</sup>) is the rate of surface water intake;  $\Delta t$  denotes the model time step.

213 The groundwater extraction process can be expressed as (Zeng et al., 2016):

$$214 \quad S_{gw}' = S_{gw} - q_{gw} \Delta t, \quad (11)$$

215 
$$h' = h - \frac{q_{gw} \Delta t}{s}, \quad (12)$$

216 where  $S_{gw}$  (mm) is the original unconfined aquifer water storage;  $q_{gw}$  (mm s<sup>-1</sup>) is the rate of  
 217 groundwater pumping;  $h$  (mm) represents the original groundwater table depth;  $s$  is the aquifer-  
 218 specific yield;  $S_{gw}'$  (mm) and  $h'$  (mm) denote the aquifer water storage and the groundwater table depth  
 219 after pumping.

220 Human water use can be divided into agricultural irrigation water and other industrial and domestic  
 221 water, where irrigation water is considered as effective precipitation directly back to the soil surface and  
 222 other water is directly added to the model surface runoff and evapotranspiration fluxes in a certain  
 223 proportion (Zou et al., 2015). This process can be estimated by the following equations:

224 
$$q_{top} = q_{top} + q_{irrig}, \quad (13)$$

225 
$$q_{surf} = q_{surf} + 0.3q_{ind} + 0.3q_{dom}, \quad (14)$$

226 
$$Q_{evap} = q_{evap} + 0.7q_{ind} + 0.7q_{dom}, \quad (15)$$

227 where  $q_{top}$  (mm s<sup>-1</sup>) is the rate of net water flow entering the soil surface;  $q_{surf}$  and  $q_{evap}$  (mm s<sup>-1</sup>) are  
 228 surface runoff and evaporation; and  $q_{irrig}$ ,  $q_{ind}$ , and  $q_{dom}$  (mm s<sup>-1</sup>) denote irrigation, industrial, and  
 229 domestic water respectively. The coefficients were set to 0.3 and 0.7 due to the limitation of data (Liu et  
 230 al., 2019; Zou et al., 2014).

## 231 2.5. DOC transfer induced by water withdrawal and use

232 Anthropogenic water regulation activities also affect DOC transport processes between land and river. It  
 233 was assumed here that (1) only the interception effect of reservoirs would be considered, ignoring the  
 234 migration transformation process in reservoirs, and the loss rate in reservoirs would be equal to that in  
 235 rivers; (2) because groundwater extraction usually occurs *in situ* and will pass through the filtering effect  
 236 of the soil layer, the part of DOC that returned to soil with groundwater extraction was ignored; (3) the  
 237 loss rate in the process of DOC returning to soil was equal to that in rivers.

238 The process of reservoir interception leading to retention of carbon in rivers can be expressed as:

239 
$$F_{DOC,r} = \frac{v(con_r \Delta Q_r)}{d}, \quad (16)$$

240 where  $F_{DOC,r}$  (kg C s<sup>-1</sup>) denotes the DOC flux retained by the reservoir;  $con_r$  (kg C m<sup>-3</sup>) is the DOC  
 241 concentration in the reservoir;  $\Delta Q_r$  (m<sup>3</sup>) is the water volume change in the reservoir.

242 The DOC flux extracted from surface water is calculated based on the intake rate and the solute



243 concentration in the current grid cell and enters the soil DOC pool after irrigation. The reduction in soil  
244 DOC leaching due to groundwater extraction is then calculated based on soil DOC concentration and  
245 groundwater pumping rate.

### 246 **3. Data and Experimental Design**

#### 247 **3.1. Data Sources**

248 The climate input forcing data set ( $0.5^\circ \times 0.5^\circ$ ) used for the model proposed in this study was obtained  
249 from CRU-NCEP Version 7 (Viovy, 2018), including air temperature, humidity, incoming solar radiation,  
250 precipitation, surface pressures, and surface winds. The basic land-surface datasets required to drive the  
251 model were set up using the default CLM 5.0 settings with a spatial resolution of  $0.9^\circ \times 1.25^\circ$ ; more  
252 details are available in the technical notes (Lawrence et al., 2018). The global monthly mean atmospheric  
253 CO<sub>2</sub> concentration dataset came from the NOAA/Earth System Research Laboratory  
254 (<https://www.esrl.noaa.gov/gmd/ccgg/trends/global.html>).

255 Reservoir information was obtained from the Global Reservoir and Dam Database (GRanD, Lehner et  
256 al., 2011), containing information on 6,862 dams and their associated reservoirs worldwide, and  
257 interpolated to a spatial resolution of  $0.5^\circ \times 0.5^\circ$  (Fig.S2).

258 The human water use activity dataset was derived from the global long-term surface and groundwater  
259 withdrawal dataset estimated by Liu et al. (2019). The dataset has a spatial resolution of  $0.5^\circ \times 0.5^\circ$  and  
260 contains agricultural, industrial, and domestic water demands from 1958 to 2017. It was derived based  
261 on five datasets: the water use dataset from the Food and Agricultural Organization (FAO), a shape file  
262 data of national boundaries, the Global Map of Irrigation Areas, version 5 (GAMIP5; Siebert et al., 2013),  
263 the historical monthly soil moisture levels and saturated soil moisture levels (Zeng et al., 2017), and the  
264 FAO water information system for 2010, which contained the agricultural, industrial, and municipal  
265 water withdrawals.

#### 266 **3.2. Observation Data**

267 Because there are few datasets of long time-series observations of DOC fluxes for large global rivers,  
268 annual averages were used to validate the model simulations. The dataset was derived from the database  
269 developed by Dai et al. (2012), which provides discharge and DOC flux observations for sites on the

270 world's major large rivers. These sites were globally distributed and were influenced by various climatic  
 271 and human activities.

**Table 1.** Summary of the main datasets used in this study

<u>Dataset</u>	<u>Resolution</u>	<u>Time period</u>	<u>Data Source</u>
<u>CRU-NCEP V7 forcing</u>	<u>0.5°/6 hr</u>	<u>1981-2013</u>	<u>Viovy (2018)</u>
<u>Surface water and groundwater withdrawal and use</u>	<u>0.5°</u>	<u>1958-2017</u>	<u>Liu et al. (2019)</u>
<u>Reservoir information</u>	<u>Site</u>	<u>Around 2011</u>	<u>Lehner et al. (2011)</u>
<u>River discharge</u>	<u>Site</u>	<u>Annual before 2009</u>	<u>Dai et al. (2012)</u>
<u>DOC export</u>	<u>Site</u>	<u>Annual before 2009</u>	<u>Dai et al. (2012)</u>

### 272 3.3. Experimental Design

273 To investigate the effect of anthropogenic water regulation on DOC transport in rivers, three sets of  
 274 simulations were designed using the developed model (Table 1). The first simulation (CTL) was a control  
 275 experiment without considering any anthropogenic water regulation activities. The second simulation  
 276 (EXPA) only considered surface water regulation, and the last simulation (EXPB) considered all  
 277 anthropogenic water regulation. All simulations were run from 1981 to 2013 with a spatial resolution of  
 278  $0.9^\circ \times 1.25^\circ$  for the land-surface module and  $0.5^\circ \times 0.5^\circ$  for the RTM. The results were output on a  
 279 monthly scale. Before the formal numerical simulations, the 1901–1920 atmospheric forcing data cycle  
 280 was used to drive the model without any anthropogenic water regulation as the spin-up run to reach an  
 281 equilibrium state.

**Table 2.** Experimental design

<u>Name</u>	<u>Period</u>	<u>Surface regulation</u>	<u>Groundwater regulation</u>
CTL	1981–2013	✘	✘
EXPA	1981–2013	✓	✘
EXPB	1981–2013	✓	✓

## 282 4. Results

### 283 4.1. Model Evaluation

284 Figure 2 shows the spatial distribution of multi-year average soil DOC losses, which are the sum of DOC  
 285 surface runoff and subsurface leaching. The results show that the global distribution of soil DOC losses  
 286 varied widely, especially in Russia and Southeast Asia, western Africa, and tropical South America,

删除了: 1

287 where the losses exceeded  $1.8 \times 10^4 \text{ kg C km}^{-2} \text{ yr}^{-1}$ , whereas low runoff arid regions such as northwestern  
288 China, India, and North Africa had the smallest soil DOC losses. The tropics and the temperate regions  
289 of the Northern Hemisphere were the regions with the highest soil DOC losses, which is generally  
290 consistent with previous studies (Harrison et al., 2005).

删除了: 8,000

设置了格式: 上标

删除了: was

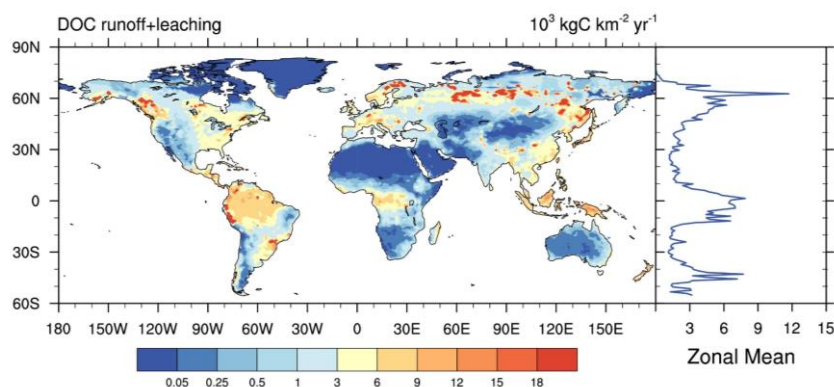


**Figure 2.** Spatial distribution and zonal mean of multi-year average soil DOC losses from 1981 to 2013.

291 The multi-year average river discharges and DOC export fluxes simulated by the developed model  
292 were then compared with observed data. Because the model resolution was  $0.5^\circ \times 0.5^\circ$ , only 106 rivers  
293 with watershed areas larger than  $2,500 \text{ km}^2$  were selected. The simulated river discharges were slightly  
294 underestimated (Fig. 3c), but fit well with observations (Fig. 3a) and provided a solid basis for subsequent  
295 simulation of river carbon exports. In addition, the simulated riverine DOC export fluxes tended to be  
296 overestimated in temperate regions and underestimated in the tropics (Fig. 3d), but were close to the 1:1  
297 line compared to the observed DOC fluxes, with  $R^2$  reaching 0.61 and significantly correlated (Fig. 3b).  
298 Moreover, the total global river DOC export fluxes simulated by the proposed model were compared  
299 with the results of previous studies. We estimated that the global terrestrial ecosystem delivers about  
300  $199.78 \pm 36.63$  ( $\pm 1$  standard deviation) Tg of DOC per year to the ocean via rivers, which was in the  
301 middle of the values derived from previous studies (Table 2). Therefore, it could be believed that the  
302 model has reasonable accuracy and can be applied to global-scale riverine DOC export simulation studies.

删除了: overestimated

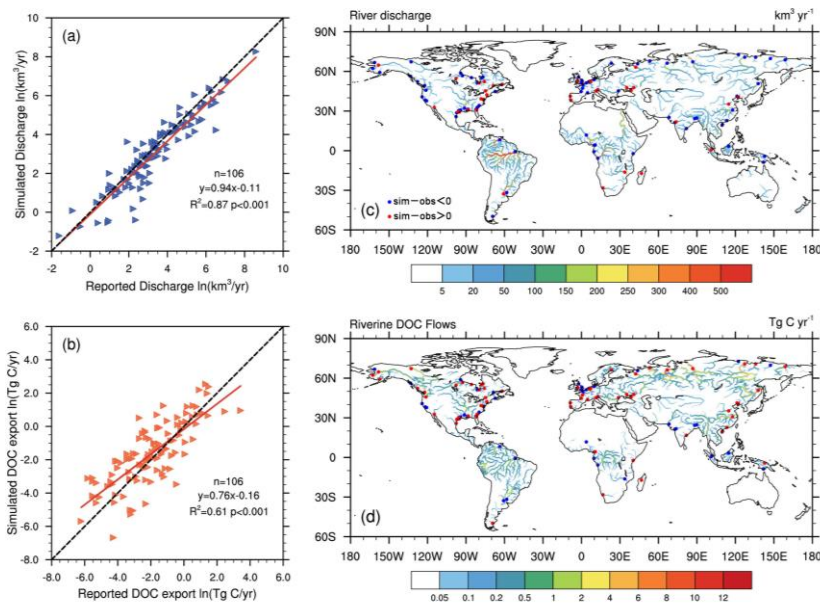


**Figure 3.** Simulated and reported annual (a) river discharge and (b) riverine DOC export flux for 106 global rivers. Spatial distributions of (c) annual discharge and (d) annual riverine DOC exports during 1981–2013. The dots in the map correspond to the locations of the 106 river sites, where blue dots indicate sites that are simulated underestimates and red dots indicate sites that are simulated overestimates.

**Table 3.** Comparison of simulated global total riverine DOC export fluxes with previous studies

Method	DOC (Tg C yr <sup>-1</sup> )	Data Source
GEMS-GLORI	215	Meybeck (1982)
Empirical model	204	Smith & Hollibaugh (1993)
Empirical model	204.81	Ludwig et al. (1996)
Global C: N	361	Aitkenhead & McDowell (2000)
NEWS-DOC	170	Harrison et al. (2005)
Global-NEWS	170	Seitzinger et al. (2005)
Statistical estimation	246	Cai (2011)
<u>Statistical estimation</u>	<u>232.22</u>	<u>Drake et al. (2018)</u>
TRIPLEX-HYDRA	240	Li et al. (2019)
Empirical model	131.6	Fabre et al. (2020)
<u>DISC-CARBON</u>	<u>132</u>	<u>van Hoek et al. (2021)</u>
CLM5.0-RTM	199.78	This study

删除了:

删除了: 2

删除了:(

删除了,;

删除了:(

删除了,;

#### 306 4.2. Effects of surface water regulation on riverine DOC transport

307 The difference between EXPA and CTL was used to obtain the effect of surface water regulation on land

带格式的: 不取消行号

308 surface hydrological variables. Surface water use has resulted in changes in latent and sensible heat fluxes  
 309 in most global irrigation water-using regions (Fig. 4a, 4b), especially in arid or semi-arid regions such as  
 310 northern China, India, and the central United States, where latent heat fluxes have increased and sensible  
 311 heat fluxes have decreased. Soil and surface temperatures in these regions have also decreased due to the  
 312 cooling effect of irrigation (Fig. 4c, 4d). Figure 4e shows that irrigation led to an overall increase in soil  
 313 moisture, especially in northern India, Western Europe, and the midwestern United States. In addition,  
 314 irrigation also led to an increase in total runoff (Fig. 4f).

删除了:

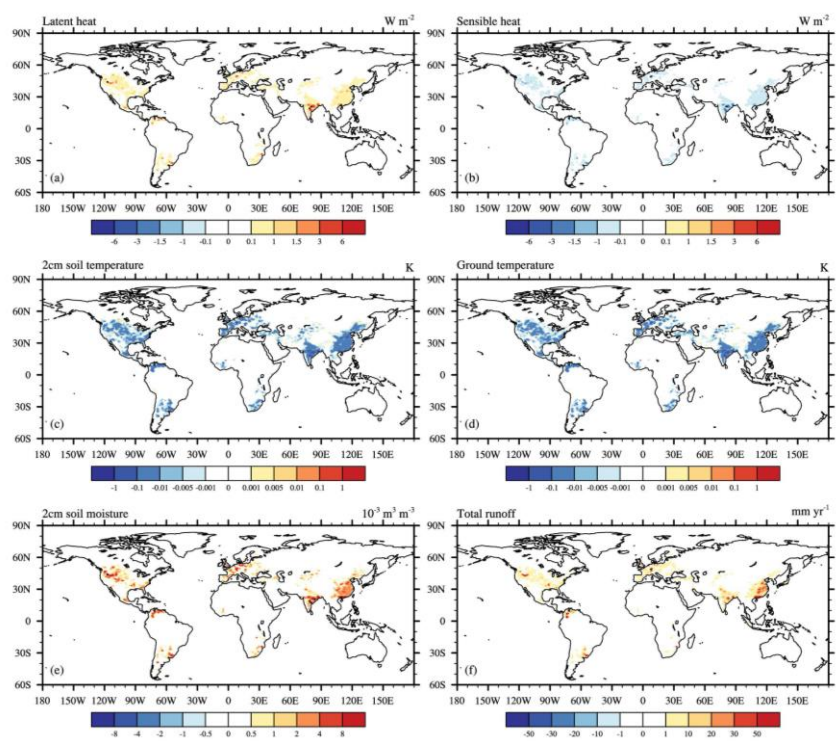


**Figure 4.** Spatial distribution of multi-year average differences in land surface hydrological variables between EXPA and CTL from 1981 to 2013; (a) latent heat flux, (b) sensible heat flux, (c) 2 cm soil temperature, (d) surface temperature, (e) 2 cm soil moisture, (f) total runoff. This figure demonstrates the effects of surface water regulation on land surface hydrological variables. The black dots are the regions that pass the significance *t*-test at the 95 % confidence level.

删除了: changes

删除了: due to surface water regulation from 1981 to 2013

删除了: The

315 Figures 5a and 5b display the effects of surface water regulation on soil carbon losses. Specifically,  
 316 the hotspots of significantly increased surface DOC runoff were in areas of high agricultural influence,

带格式的: 缩进: 首行缩进: 1 字符, 不取消行号

318 such as the central United States, northern India, and northern and eastern China, reaching up to 2,000  
 319 kg C km<sup>-2</sup> yr<sup>-1</sup>, but the increase in subsurface leaching was relatively small. This may have been the case  
 320 because surface water withdrawals from rivers and reservoirs were returned to the soil by irrigation,  
 321 bringing back some DOC, directly increasing surface runoff, and also increasing subsurface runoff, and  
 322 thus increasing soil DOC losses.

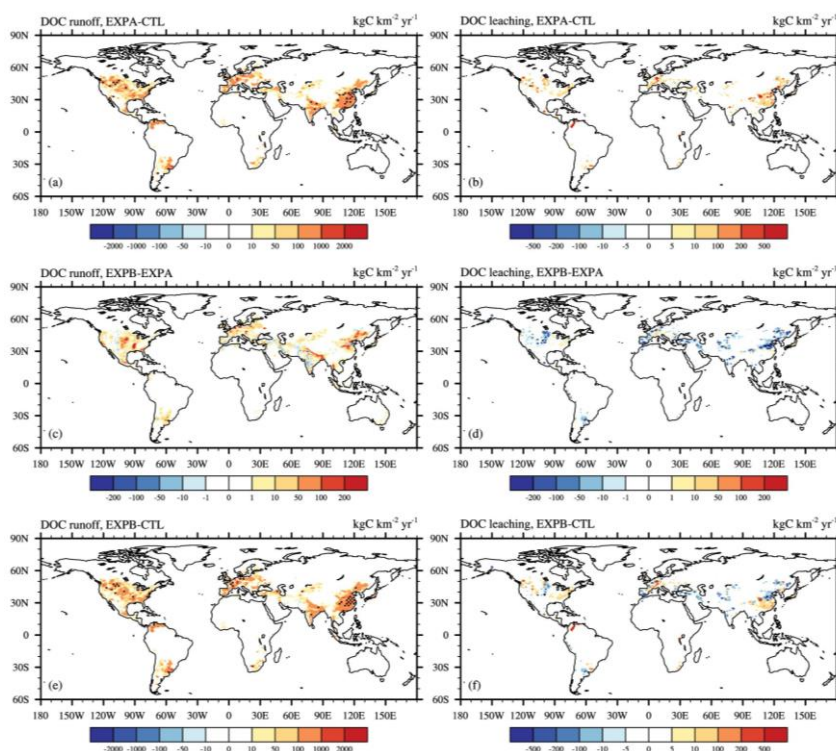


**Figure 5.** Spatial distribution of the multi-year average differences between different experiments from 1981 to 2013 in the (a) soil DOC runoff, EXPB-CTL, (b) soil DOC leaching, EXPB-CTL, (c) soil DOC runoff, EXPB-EXPA, (d) soil DOC leaching, EXPB-EXPA, (e) soil DOC runoff, EXPB-CTL, (f) soil DOC leaching, EXPB-CTL. This figure demonstrates the effects of (a, b) surface water regulation, (c, d) groundwater regulation, and (e, f) anthropogenic water regulation on soil DOC losses. The black dots are the regions that pass the significance *t*-test at the 95 % confidence level.

323 From Fig. 6a and Fig. 6b, surface water regulation had a significant effect on river discharge and  
 324 riverine DOC flow. The combined effects of reservoir interception and surface water withdrawal reduced  
 325 the discharge and DOC export of most rivers globally, with significant reductions of more than 50 Gg C  
 326 yr<sup>-1</sup> in the Yangtze, Yellow, Mississippi, and Ganges Rivers and in some basins in Western Europe. Some

删除了:

删除了:

删除了: multi-year average changes in soil carbon losses due to

删除了: surface water regulation

设置了格式: 非上标/下标

删除了: (a, b),

删除了: groundwater regulation (c, d), and

删除了: anthropogenic water regulation

删除了: (e, f) from 1981 to 2013

328 rivers in northern South America experienced increased riverine DOC export, but not significantly,  
 329 probably because the increase in river flow caused by agricultural irrigation could have been greater than  
 330 the decrease caused by surface water regulation.

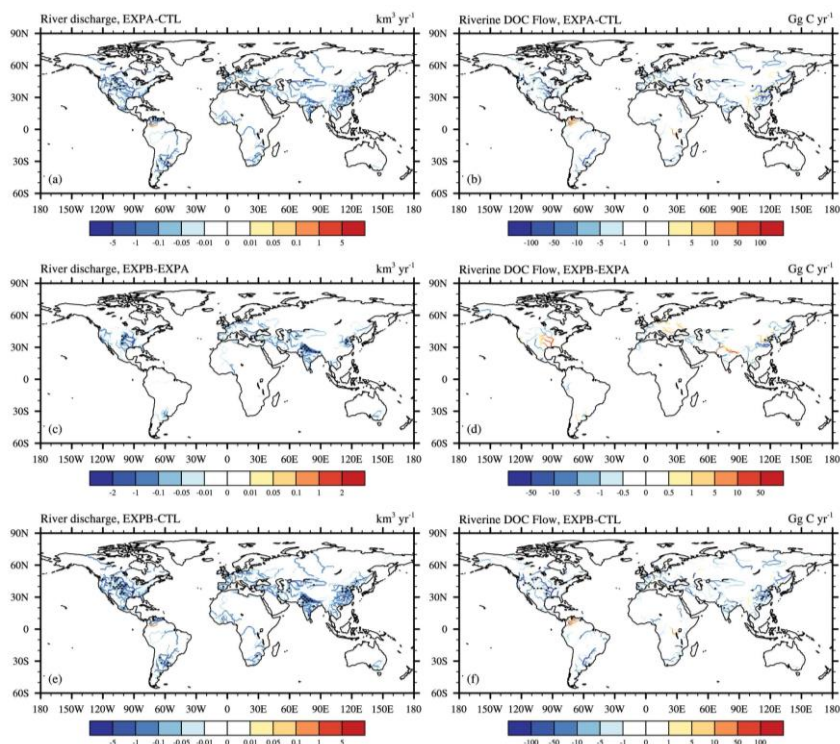


**Figure 6.** Spatial distribution of the multi-year average differences between different experiments from 1981 to 2013 in the (a) river discharge, EXPA-CTL, (b) riverine DOC flow, EXPA-CTL, (c) river discharge, EXPB-EXPA, (d) riverine DOC flow, EXPB-EXPA (e) river discharge, EXPB-CTL, (f) riverine DOC flow, EXPB-CTL. This figure demonstrates the effects of (a, b) surface water regulation, (c, d) groundwater regulation, and (e, f) anthropogenic water regulation on the river discharge and riverine DOC flow rate. The black dots are the regions that pass the significance *t*-test at the 95 % confidence level.

331 The blue line in Fig. 7 represents the time-series variation of surface water regulation on global riverine  
 332 organic carbon to the ocean. Surface water regulation greatly reduced global riverine DOC transport to  
 333 the ocean, from  $-11.1 \text{ Tg yr}^{-1}$  in 1981 to  $-16.4 \text{ Tg yr}^{-1}$  in 2013 (Fig. 7a), with a multi-year average  
 334 retention efficiency of about 6 %. This may be related to the fact that the reservoir adjusting the river  
 335 discharge and intercepting the riverine DOC. The regions most affected by surface water regulation were

删除了: Spatial distribution of multi-year average changes in river discharge and riverine DOC flow due to surface water regulation (a, b), groundwater regulation (c, d), and anthropogenic water regulation (e, f) from 1981 to 2013.

带格式的: 缩进: 首行缩进: 1 字符, 行距: 1.5 倍行距, 不取消行号

删除了: This may be related to the fact that reservoir interception increases the residence time of water and thus increases DOC removal rate (Liu et al., 2022).

339 the Pacific and Atlantic Oceans, and as surface water use in these regions became more frequent, the  
 340 reduction in DOC delivery to the ocean was intensified each year. There was no significant change in the  
 341 Arctic Ocean region, which may have been due to less anthropogenic disturbance in this area.

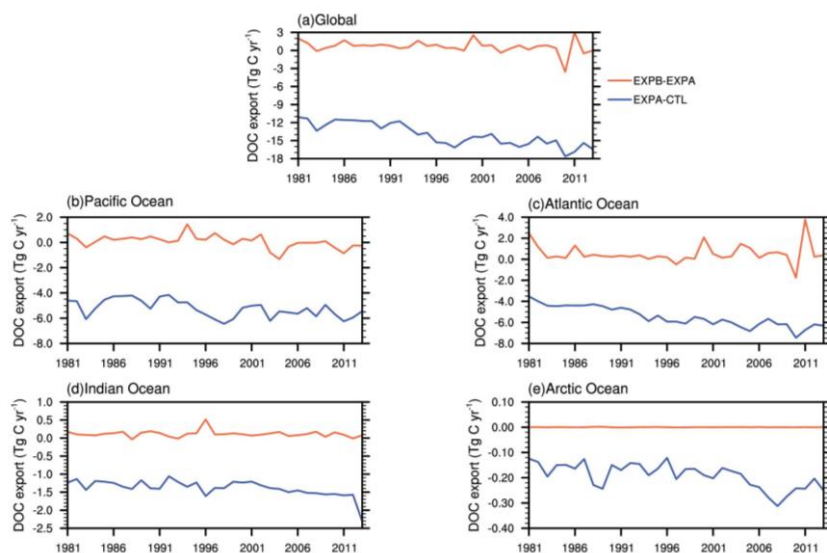


**Figure 7.** Time series of changes in DOC export to oceans due to surface water (blue line) and groundwater regulation (orange line) from 1981 to 2013: (a) global, (b) Pacific Ocean, (c) Atlantic Ocean, (d) Indian Ocean, (e) Arctic Ocean.

### 342 4.3. Effects of groundwater regulation on riverine DOC transport

343 The effects of groundwater regulation on land surface hydrological variables were obtained using the  
 344 difference between EXPB and EXPA, as shown in Fig. 8. It can be seen that groundwater extraction  
 345 increased latent heat fluxes, decreased sensible heat fluxes, decreased soil and surface temperatures, and  
 346 increased soil moisture in most regions of the world. The most significant impacts were in northern China,  
 347 northern India, Pakistan, and the central United States, where climate conditions are dry and groundwater  
 348 extraction is frequent. Unlike surface water regulation, groundwater extraction has a negative impact on  
 349 total runoff (Fig. 8f). Because groundwater is extracted from underground aquifers, whereas surface  
 350 water is extracted from rivers and reservoirs, surface water use directly increases total land surface runoff.  
 351 However, the impact of groundwater extraction on runoff depends on the groundwater pumping rate,  
 352 infiltration rate, and soil evaporation capacity. The increase in latent heat flux leads to an increase in

删除了: he alpine  
 删除了: region  
 删除了:

带格式的: 不取消行号



356

surface evapotranspiration, which results in a decrease in runoff.

删除了:

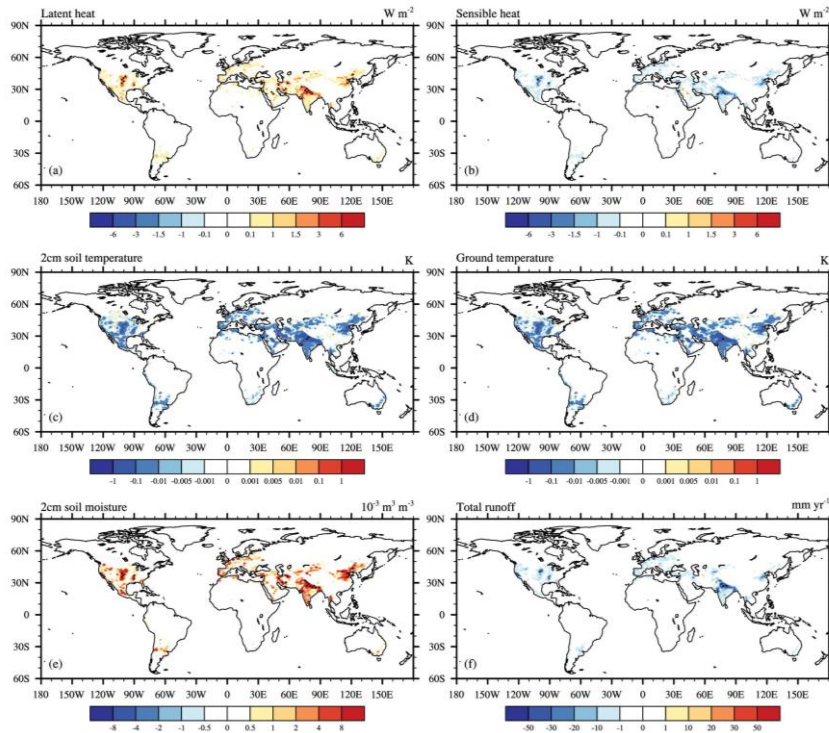


**Figure 8.** Spatial distribution of multi-year average differences in land surface hydrological variables between EXPB and EXPA from 1981 to 2013: (a) latent heat flux, (b) sensible heat flux, (c) 2 cm soil temperature, (d) surface temperature, (e) 2 cm soil moisture, (f) total runoff. This figure demonstrates the effects of groundwater regulation on land surface hydrological variables. The black dots are the regions that pass the significance *t*-test at the 95 % confidence level.

删除了: changes

删除了: due to groundwater regulation

357 Figures 5c and 5d show the effect of groundwater regulation on soil carbon losses. On the one hand,  
 358 extracting water from underground aquifers led to a reduction in subsurface runoff and a consequent  
 359 reduction in DOC leaching, especially in northern China and the central United States, where DOC  
 360 leaching reductions reached 200 kg C yr<sup>-1</sup>. On the other hand, groundwater irrigation led to an increase  
 361 in surface runoff, which led to an increase in DOC runoff. The most affected areas are characterized by  
 362 well-developed agriculture.

363 Figures 6c and 6d show the spatial distribution of the effects of groundwater regulation on river  
 364 discharge and DOC export from 1981 to 2013. It can be seen that river discharge significantly decreased  
 365 in areas with high groundwater extraction rates, such as the central United States, Pakistan, Afghanistan,

367 and northern China, resulting in a decrease in riverine DOC export. The largest decrease occurred in the  
368 Yangtze River Basin in China, reaching 50 Gg C yr<sup>-1</sup>; most other rivers were around 10 Gg C yr<sup>-1</sup>. In  
369 addition, although river discharge was reduced in some river sections, soil DOC loss was higher, and  
370 DOC export fluxes were still increasing, especially in the lower Yellow River, Mississippi River, and  
371 Ganges River basins. This was due to the predominance of agricultural irrigation water in these regions.

372 The amount of carbon flux variation influenced by groundwater regulation was relatively small  
373 compared to that influenced by surface water regulation, but there was some interannual fluctuation, with  
374 the greatest impact during 2009–2012 (Fig. 7). The intermittent increase and decrease of the variation  
375 indicate that river carbon transport fluxes did not decrease directly with increases of groundwater  
376 pumping rate, but were also related to the complex carbon and nitrogen cycling processes in terrestrial  
377 ecosystems. In addition, irrigation after groundwater extraction from an underground aquifer did not  
378 consider directly sending DOC back to the soil carbon pool, and therefore the carbon flux changes were  
379 smaller. Because groundwater regulation activities are mostly concentrated in the northern temperate  
380 zone, the Pacific and Atlantic regions were the most obviously affected, whereas the remaining regions  
381 did not change much.

#### 382 **4.4. Effects of anthropogenic water regulation on riverine DOC transport**

383 This section discusses the combined effects of anthropogenic water regulation on soil and riverine carbon  
384 transport using the EXPB minus CTL results. The effects of anthropogenic water regulation on total  
385 runoff both increased and decreased globally (Fig. 9f). The western United States, Venezuela, and  
386 northern China showed an increase in runoff due to the high intensity of irrigation water use in agriculture.  
387 In contrast, regions such as northern India and the central United States showed a decrease in runoff due  
388 to frequent groundwater extraction. Overall, human water regulation activities led to an increase in latent  
389 heat fluxes and soil moisture and a decrease in sensible heat fluxes and in soil and ground temperatures.

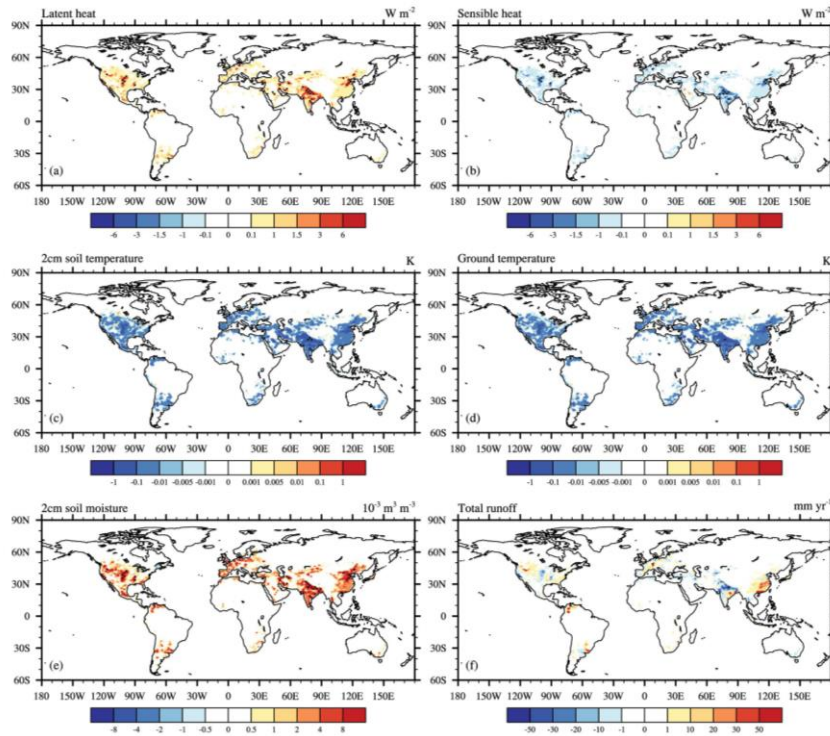


**Figure 9.** Spatial distribution of multi-year average differences in land surface hydrological variables between EXPB and CTL from 1981 to 2013: (a) latent heat flux, (b) sensible heat flux, (c) 2 cm soil temperature, (d) surface temperature, (e) 2 cm soil moisture, (f) total runoff. This figure demonstrates the effects of anthropogenic water regulation on land surface hydrological variables. The black dots are the regions that pass the significance *t*-test at the 95 % confidence level.

删除了: changes  
 删除了: due to anthropogenic water regulation

390 Figure 5e shows that soil DOC runoff increased, especially in northern China and the midwestern  
 391 United States. DOC leaching decreased in some river sections (Fig. 5f), but not significantly. Although  
 392 soil DOC runoff showed an overall increase, DOC export fluxes decreased in most rivers globally due to  
 393 water regulation (Fig. 6f). On the one hand, human water use activities led to a decrease in river discharge  
 394 (Fig. 6e), and on the other hand, reservoirs have intercepted part of riverine DOC, which led to an increase  
 395 in microbial activity, resulting in a decrease in river carbon flux. In contrast, in the Mississippi and  
 396 Ganges River basins, although groundwater regulation increased their DOC export fluxes (Fig. 6d), they  
 397 still showed a decrease under the negative feedback effect of surface water regulation, indicating that  
 398 most rivers globally are mainly influenced by reservoir interception and surface water withdrawal.

399 Five typical rivers were selected to exhibit how anthropogenic water regulation affects monthly and  
400 annual average DOC flows in rivers. The selected rivers were the Mississippi River in the United States,  
401 the Danube River in Europe, the Ob River in Russia, the Yangtze River in China, and the Ganges River  
402 in India. Figure 10 displays the seasonal and interannual variation of DOC flow rates in the five rivers as  
403 calculated by the three sets of simulations respectively. Anthropogenic water regulation had a significant  
404 impact on the Mississippi, Danube, Yangtze, and Ganges Rivers, which decreased significantly in winter  
405 and early spring, whereas the Ob River was almost unaffected. This was the case because of weak water  
406 management activities in the Ob River, whereas the other subtropical and temperate rivers had intense  
407 water management activities and significant seasonal variation in runoff. In addition, only the Mississippi,  
408 Yangtze, and Ganges rivers were affected by minor groundwater regulation, usually occurring during dry  
409 periods, whereas in most seasons, the rivers were affected only by surface water regulation (including  
410 reservoir interception). The annual results showed a significantly strengthening trend of riverine DOC  
411 reduction due to the influence of anthropogenic water regulation, especially in the Danube and Yangtze  
412 Rivers, where the retention percentage in 2013 was four to five times higher than in 1981, up to more  
413 than 50 %, indicating a clear intensification of human water management activities. The influence on the  
414 Mississippi and Ganges Rivers increased slightly and stabilized at about 30–40 %, whereas the influence  
415 on the Ob River was almost 0.

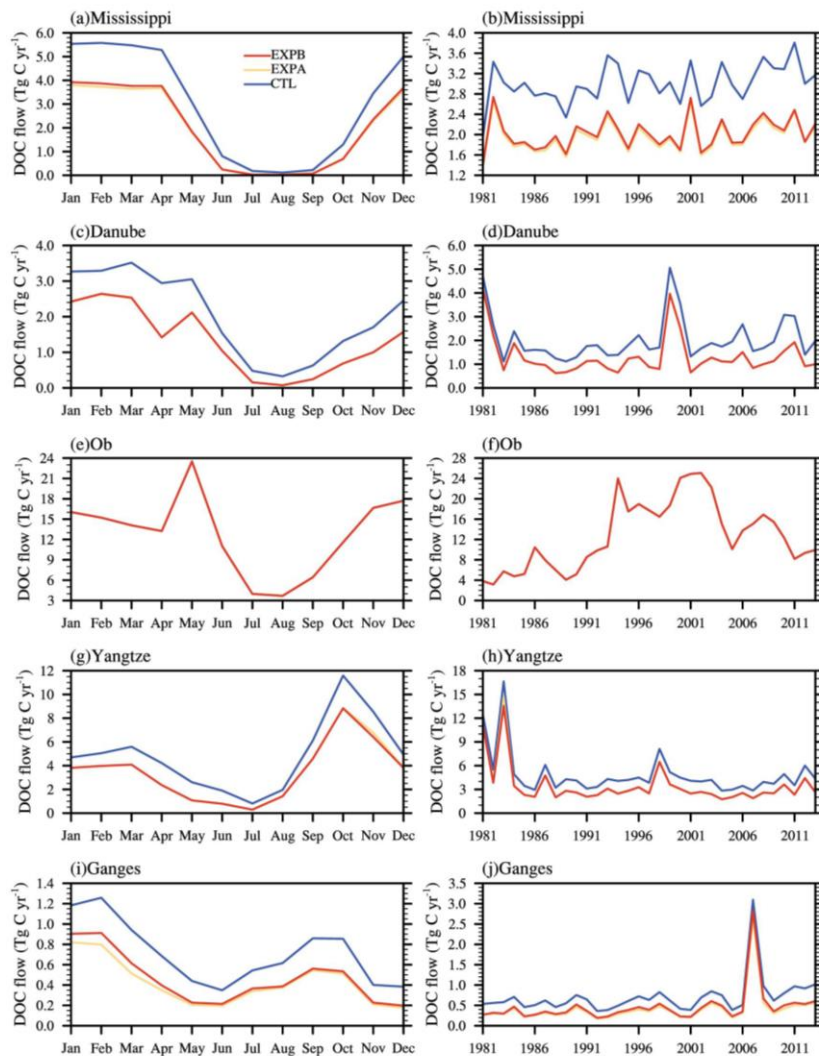


**Figure 10.** Time series of (a, c, e, g, i) monthly and (b, d, f, h, j) annual average riverine DOC flow rates for the five typical rivers simulated by CTL (blue line), EXPA (yellow line), and EXPB (red line): (a, b) Mississippi River (32.25° N, 91.25° W), (c, d) Danube River (45.25° N, 28.75° E), (e, f) Ob River (66.25° N, 66.75° E), (g, h) Yangtze River (30.75° N, 117.75° E), (i, j) Ganges River (24.25° N, 88.25° E).

416 Riverine DOC export fluxes have obvious spatial heterogeneity. Six zones were defined according to  
 417 the latitudes where the river mouths are located, and the effects of the presence or absence of  
 418 anthropogenic water regulation on DOC export fluxes are shown in Fig. 11. The hotspot regions of

419 riverine DOC export are concentrated in the tropics (23.5° S–23.5° N) and the mid and high latitudes of  
 420 the Northern Hemisphere (40–90° N). The DOC export fluxes of rivers between 40° N and 66° N  
 421 accounted for 35.32 % of total global export flux. Due to anthropogenic water regulation, the global DOC  
 422 export flux was reduced by  $13.36 \pm 2.45$  Tg C yr<sup>-1</sup> compared to the case with no human regulation, with  
 423 the greatest impact concentrated in the subtropical and temperate regions of the Northern Hemisphere  
 424 (23.5–66° N) because this is the region with the highest intensity of human water use activity.

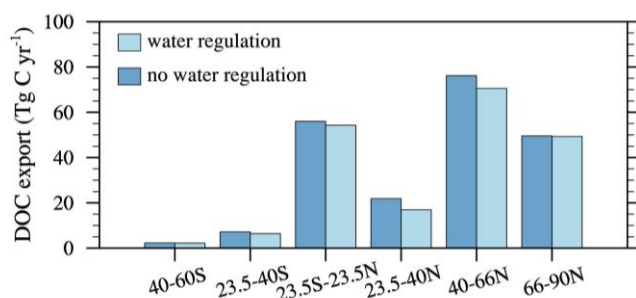


**Figure 11.** Bar chart of latitudinal band distribution of multi-year average DOC export fluxes from 1981 to 2013. Dark blue indicates no water regulation, and light blue indicates anthropogenic water regulation.

删除了: human activity

425 Overall, anthropogenic water regulation reduced global riverine carbon fluxes, and the reduction in  
 426 DOC fluxes also intensified over time, from  $-9.13$  Tg C yr<sup>-1</sup> to  $-16.45$  Tg C yr<sup>-1</sup> (Fig. 12), and the  
 427 reduction percentage also increased from 4.83 % to 6.20 %. Rivers in the Pacific and Atlantic regions  
 428 were more affected by water regulation, and the interannual changes were more consistent with the global  
 429 picture. The flux of rivers into the Indian Ocean, which was reduced by water regulation, was about  $1.27$   
 430  $\pm 0.23$  Tg C yr<sup>-1</sup>, which was small compared to the global flux, and the flux into the Arctic Ocean was  
 431 almost negligible due to the scarcity of human activities.

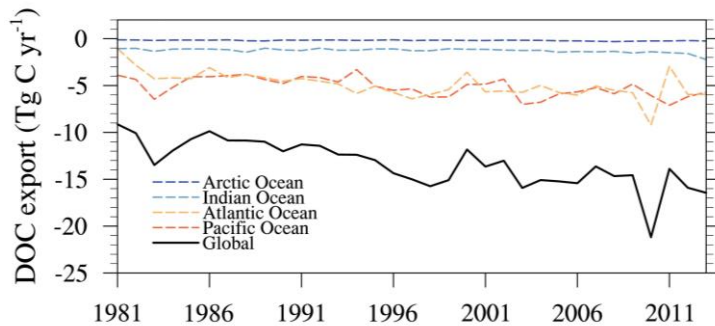


**Figure 12.** Interannual variability in the impact of anthropogenic water regulation on riverine DOC delivery from rivers to the ocean.

## 432 5. Conclusions

433 This study has developed schemes that consider soil and riverine DOC dynamics and anthropogenic  
 434 water regulation activities and has incorporated them into the land surface model CLM5.0. The simulated  
 435 river discharges and riverine DOC export fluxes were in good agreement with observations obtained for  
 436 106 major world rivers. Surface water and groundwater use datasets were used as inputs to the model,  
 437 and three sets of numerical simulations were conducted from 1981 to 2013 on a global scale to investigate  
 438 the effects of anthropogenic water regulation on riverine DOC transport.

439 The main conclusions of this study are as follows. First, anthropogenic water regulation activities  
 440 increased soil losses in most arid and semi-arid regions of the world, although groundwater extraction  
 441 reduced subsurface runoff and decreased DOC leaching; however, this decrease was less than the increase  
 442 in DOC runoff due to irrigation. Second, the DOC export fluxes of the Yangtze, Yellow, Mississippi, and  
 443 Ganges River basins were significantly reduced by reservoir regulation and surface water withdrawal.  
 444 However, DOC export fluxes in these areas showed an increase under groundwater regulation, but the  
 445 increase was small, indicating that DOC transport in most rivers globally is mainly influenced by  
 446 reservoir interception and surface water regulation. Third, further analysis showed that subtropical and  
 447 temperate rivers with intensive water management regimes were more affected and that DOC flows  
 448 decreased substantially in winter and early spring. The retention percentage has been increasing year by  
 449 year, up to over 50 %, indicating a clear intensification of human water management activities, especially  
 450 along the Danube and Yangtze Rivers. In addition, the greatest impact of anthropogenic water regulation

451 activities was concentrated in the region from 23.5°N to 66°N because this zone contains the highest  
452 intensity of human water use activities. Fourth, global riverine DOC flux transport to the ocean decreased  
453 by an average of  $13.36 \pm 2.45$  Tg C yr<sup>-1</sup> per year due to anthropogenic water regulation activities, and  
454 the decrease in DOC flux became more pronounced with time, from -9.13 Tg C yr<sup>-1</sup> (4.83 %) in 1981 to  
455 -16.45 Tg C yr<sup>-1</sup> (6.20 %) in 2013, especially in the Pacific and Atlantic Ocean regions. Meanwhile, the  
456 Arctic Ocean region was almost unaffected due to low anthropogenic disturbance. In general, this study  
457 has developed an effective scheme to simulate DOC export from terrestrial to aquatic systems, which is  
458 important for improving carbon budget estimation and integrated ecosystem management.

459 However, there are still some limitations and uncertainties in the developed model that need to be  
460 addressed in the future. In this study, we evaluated global riverine DOC transport using observations  
461 from a limited number of river sites in literature records, which may have induced a bias. Besides, the  
462 simplification of the carbon dynamics of soils and rivers, the uniform parameters, and input data sets also  
463 produce some uncertainties. To advance the current model, more observed data sets and more complex  
464 schemes of carbon dynamics are needed. In addition, other human activities, such as fertilization,  
465 wastewater discharge, and land use change, have a significant impact on riverine carbon transport  
466 (Regnier et al., 2013), and should be considered in our future work.

467  
468 **Code and Data Availability.** The observed river discharge and riverine DOC exports data can be available  
469 through Dai et al. (2012). The source code of CLM 5.0 is available online  
470 (<https://www.cesm.ucar.edu/models/clm>). The FORTRAN code of developed model in this study is  
471 available upon request. Please contact Zhenghui Xie at [zxie@lasg.iap.ac.cn](mailto:zxie@lasg.iap.ac.cn). The drawing language is the  
472 NCL language.

473  
474 **Author contributions.** The scientific framing of this paper was developed by YY, ZX, BJ. The model  
475 was initiated by YY and YW. The literature review was performed by HY, YT and SC. Analyses and  
476 scientific post-processing were performed by LW and RL. All authors discussed the results and  
477 contributed to the writing of the paper.

478  
479 **Competing interests.** The contact author has declared that neither they nor their co-authors have any  
480 competing interests.

删除了:



482

483 *Acknowledgements.* This work was jointly supported by the National Natural Science Foundation of  
484 China (grant number: 41830967), the National Key Research and Development Program of China (grant  
485 number: 2022YFC3201903), ~~the Youth Innovation Promotion Association CAS (2021073), and the~~  
486 ~~National Natural Science Foundation of China (grant number: 42175163).~~

删除了: and

488 **References**

- 489 Aitkenhead, J. A. and McDowell, W. H.: Soil C:N ratio as a predictor of annual riverine DOC flux at  
490 local and global scales, *Global Biogeochem. Cycles*, 14, 127–138,  
491 <https://doi.org/10.1029/1999GB900083>, 2000.
- 492 Cai, W.: Estuarine and Coastal Ocean Carbon Paradox: CO<sub>2</sub> Sinks or Sites of Terrestrial Carbon  
493 Incineration?, *Annu. Rev. Mar. Sci.*, 3, 123–145, <https://doi.org/10.1146/annurev-marine-120709-142723>, 2011.
- 495 Camino-Serrano, M., Guenet, B., Luyssaert, S., Ciais, P., Bastrikov, V., De Vos, B., Gielen, B., Gleixner,  
496 G., Jornet-Puig, A., Kaiser, K., Kothawala, D., Lauerwald, R., Peñuelas, J., Schrumppf, M., Vicca, S.,  
497 Vuichard, N., Walmsley, D., and Janssens, I. A.: ORCHIDEE-SOM: modeling soil organic carbon (SOC)  
498 and dissolved organic carbon (DOC) dynamics along vertical soil profiles in Europe, *Geosci. Model Dev.*,  
499 11, 937–957, <https://doi.org/10.5194/gmd-11-937-2018>, 2018.
- 500 Cole, J. J., Prairie, Y. T., Caraco, N. F., McDowell, W. H., Tranvik, L. J., Striegl, R. G., Duarte, C. M.,  
501 Kortelainen, P., Downing, J. A., Middelburg, J. J., and Melack, J.: Plumbing the Global Carbon Cycle:  
502 Integrating Inland Waters into the Terrestrial Carbon Budget, *Ecosystems*, 10, 172–185,  
503 <https://doi.org/10.1007/s10021-006-9013-8>, 2007.
- 504 Dai, M., Yin, Z., Meng, F., Liu, Q., and Cai, W.-J.: Spatial distribution of riverine DOC inputs to the  
505 ocean: an updated global synthesis, *Current Opinion in Environmental Sustainability*, 4, 170–178,  
506 <https://doi.org/10.1016/j.cosust.2012.03.003>, 2012.
- 507 Drake, T. W., Raymond, P. A., and Spencer, R. G. M.: Terrestrial carbon inputs to inland waters: A current  
508 synthesis of estimates and uncertainty, *Limnol Oceanogr Lett*, 3, 132–142,  
509 <https://doi.org/10.1002/lo12.10055>, 2018.
- 510 Fabre, C., Sauvage, S., Probst, J.-L., and Sánchez-Pérez, J. M.: Global-scale daily riverine DOC fluxes  
511 from lands to the oceans with a generic model, *Global and Planetary Change*, 194, 103294,  
512 <https://doi.org/10.1016/j.gloplacha.2020.103294>, 2020.
- 513 Futter, M. N., Butterfield, D., Cosby, B. J., Dillon, P. J., Wade, A. J., and Whitehead, P. G.: Modeling the  
514 mechanisms that control in-stream dissolved organic carbon dynamics in upland and forested catchments:  
515 MODELING SURFACE WATER DOC, *Water Resour. Res.*, 43,  
516 <https://doi.org/10.1029/2006WR004960>, 2007.
- 517 Gerber, S., Hedin, L. O., Oppenheimer, M., Pacala, S. W., and Shevliakova, E.: Nitrogen cycling and  
518 feedbacks in a global dynamic land model, *Global Biogeochem. Cycles*, 24,  
519 <https://doi.org/10.1029/2008GB003336>, 2010.
- 520 Gommet, C., Lauerwald, R., Ciais, P., Guenet, B., Zhang, H., and Regnier, P.: Spatiotemporal patterns  
521 and drivers of terrestrial dissolved organic carbon (DOC) leaching into the European river network, *Earth  
522 Syst. Dynam.*, 13, 393–418, <https://doi.org/10.5194/esd-13-393-2022>, 2022.
- 523 Hanasaki, N., Kanae, S., and Oki, T.: A reservoir operation scheme for global river routing models,

524 Journal of Hydrology, 327, 22–41, <https://doi.org/10.1016/j.jhydrol.2005.11.011>, 2006.

525 Harrison, J. A., Caraco, N., and Seitzinger, S. P.: Global patterns and sources of dissolved organic matter  
526 export to the coastal zone: Results from a spatially explicit, global model: GLOBAL DISSOLVED  
527 ORGANIC MATTER EXPORT, *Global Biogeochem. Cycles*, 19, n/a-n/a,  
528 <https://doi.org/10.1029/2005GB002480>, 2005.

529 van Hoek, W. J., Wang, J., Vilmin, L., Beusen, A. H. W., Mogollón, J. M., Müller, G., Pika, P. A., Liu,  
530 X., Langeveld, J. J., Bouwman, A. F., and Middelburg, J. J.: Exploring Spatially Explicit Changes in  
531 Carbon Budgets of Global River Basins during the 20th Century, *Environ. Sci. Technol.*, 55, 16757–  
532 16769, <https://doi.org/10.1021/acs.est.1c04605>, 2021.

533 Janssens, I. A. and Pilegaard, K.: Large seasonal changes in  $Q_{10}$  of soil respiration in a beech forest:  
534 SHORT-TERM  $Q_{10}$  OF SOIL RESPIRATION, *Global Change Biology*, 9, 911–918,  
535 <https://doi.org/10.1046/j.1365-2486.2003.00636.x>, 2003.

536 Lawrence, D., Fisher, R., and Koven, C.: Technical Description of version 5.0 of the Community Land  
537 Model (CLM), NCAR, NCAR, Boulder, US, 2018.

538 Lehner, B., Liermann, C. R., Revenga, C., Vörösmarty, C., Fekete, B., Crouzet, P., Döll, P., Endejan, M.,  
539 Frenken, K., Magome, J., Nilsson, C., Robertson, J. C., Rödel, R., Sindorf, N., and Wisser, D.: High-  
540 resolution mapping of the world’s reservoirs and dams for sustainable river-flow management, *Frontiers*  
541 *in Ecology and the Environment*, 9, 494–502, <https://doi.org/10.1890/100125>, 2011.

542 Li, H., Wigmosta, M. S., Wu, H., Huang, M., Ke, Y., Coleman, A. M., and Leung, L. R.: A Physically  
543 Based Runoff Routing Model for Land Surface and Earth System Models, *Journal of Hydrometeorology*,  
544 14, 808–828, <https://doi.org/10.1175/JHM-D-12-015.1>, 2013.

545 Li, M., Peng, C., Zhou, X., Yang, Y., Guo, Y., Shi, G., and Zhu, Q.: Modeling Global Riverine DOC Flux  
546 Dynamics From 1951 to 2015, *J. Adv. Model. Earth Syst.*, 11, 514–530,  
547 <https://doi.org/10.1029/2018MS001363>, 2019.

548 Liao, C., Zhuang, Q., Leung, L. R., and Guo, L.: Quantifying Dissolved Organic Carbon Dynamics Using  
549 a Three-Dimensional Terrestrial Ecosystem Model at High Spatial-Temporal Resolutions, *J. Adv. Model.*  
550 *Earth Syst.*, 11, 4489–4512, <https://doi.org/10.1029/2019MS001792>, 2019.

551 Liu, S., Xie, Z., Zeng, Y., Liu, B., Li, R., Wang, Y., Wang, L., Qin, P., Jia, B., and Xie, J.: Effects of  
552 anthropogenic nitrogen discharge on dissolved inorganic nitrogen transport in global rivers, *Glob Change*  
553 *Biol.*, 25, 1493–1513, <https://doi.org/10.1111/gcb.14570>, 2019.

554 Liu, S., Xie, Z., Liu, B., Wang, Y., Gao, J., Zeng, Y., Xie, J., Xie, Z., Jia, B., Qin, P., Li, R., Wang, L., and  
555 Chen, S.: Global river water warming due to climate change and anthropogenic heat emission, *Global*  
556 *and Planetary Change*, 193, 103289, <https://doi.org/10.1016/j.gloplacha.2020.103289>, 2020.

557 Liu, S., Maavara, T., Brinkerhoff, C. B., and Raymond, P. A.: Global Controls on DOC Reaction Versus  
558 Export in Watersheds: A Damköhler Number Analysis, *Global Biogeochemical Cycles*, 36,  
559 <https://doi.org/10.1029/2021GB007278>, 2022.

560 Ludwig, W., Probst, J.-L., and Kempe, S.: Predicting the oceanic input of organic carbon by continental  
561 erosion, *Global Biogeochem. Cycles*, 10, 23–41, <https://doi.org/10.1029/95GB02925>, 1996.

562 Maavara, T., Lauerwald, R., Regnier, P., and Van Cappellen, P.: Global perturbation of organic carbon  
563 cycling by river damming, *Nat Commun*, 8, 15347, <https://doi.org/10.1038/ncomms15347>, 2017.

564 Meybeck, M.: Carbon, nitrogen, and phosphorus transport by world rivers, *American Journal of Science*,  
565 282, 401–450, <https://doi.org/10.2475/ajs.282.4.401>, 1982.

566 Meybeck, M. and Ragu, A.: GEMS-GLORI world river discharge database,  
567 <https://doi.org/10.1594/PANGAEA.804574>, 2012.

568 Neff, J. C. and Asner, G. P.: Dissolved Organic Carbon in Terrestrial Ecosystems: Synthesis and a Model,  
569 *Ecosystems*, 4, 29–48, <https://doi.org/10.1007/s100210000058>, 2001.

570 Oleson, K. W., Lawrence, D. M., and Bonan, G. B.: Technical Description of version 4.5 of the  
571 Community Land Model (CLM), NCAR, NCAR, Boulder, US, 2013.

572 Parton, W. J., Stewart, J. W. B., and Cole, C. V.: Dynamics of C, N, P and S in Grassland Soils: A Model,  
573 *Biogeochemistry*, 5, 109–131, <https://doi.org/10.1007/BF02180320>, 1988.

574 Regnier, P., Friedlingstein, P., Ciais, P., Mackenzie, F. T., Gruber, N., Janssens, I. A., Laruelle, G. G.,  
575 Lauerwald, R., Luysaert, S., Andersson, A. J., Arndt, S., Arnosti, C., Borges, A. V., Dale, A. W., Gallego-  
576 Sala, A., Godd ris, Y., Goossens, N., Hartmann, J., Heinze, C., Ilyina, T., Joos, F., LaRowe, D. E., Leifeld,  
577 J., Meysman, F. J. R., Munhoven, G., Raymond, P. A., Spahni, R., Suntharalingam, P., and Thullner, M.:  
578 Anthropogenic perturbation of the carbon fluxes from land to ocean, *Nature Geosci*, 6, 597–607,  
579 <https://doi.org/10.1038/ngeo1830>, 2013.

580 Ren, W., Tian, H., Cai, W.-J., Lohrenz, S. E., Hopkinson, C. S., Huang, W.-J., Yang, J., Tao, B., Pan, S.,  
581 and He, R.: Century-long increasing trend and variability of dissolved organic carbon export from the  
582 Mississippi River basin driven by natural and anthropogenic forcing: Export of DOC from the  
583 Mississippi River, *Global Biogeochem. Cycles*, 30, 1288–1299, <https://doi.org/10.1002/2016GB005395>,  
584 2016.

585 Seitzinger, S. P., Harrison, J. A., Dumont, E., Beusen, A. H. W., and Bouwman, A. F.: Sources and  
586 delivery of carbon, nitrogen, and phosphorus to the coastal zone: An overview of Global Nutrient Export  
587 from Watersheds (NEWS) models and their application., *Global Biogeochem. Cycles*, 19,  
588 <https://doi.org/10.1029/2005GB002606>, 2005.

589 Siebert, S., Henrich, V., Frenken, K., and Burke, J.: Update of the digital global map of irrigation areas  
590 to version 5., <https://doi.org/10.13140/2.1.2660.6728>, 2013.

591 Smith, S. V. and Hollibaugh, J. T.: Coastal metabolism and the oceanic organic carbon balance, *Rev.*  
592 *Geophys.*, 31, 75–89, <https://doi.org/10.1029/92RG02584>, 1993.

593 Tian, H., Yang, Q., Najjar, R. G., Ren, W., Friedrichs, M. A. M., Hopkinson, C. S., and Pan, S.:  
594 Anthropogenic and climatic influences on carbon fluxes from eastern North America to the Atlantic

595 Ocean: A process-based modeling study, *J. Geophys. Res. Biogeosci.*, 120, 757–772,  
596 <https://doi.org/10.1002/2014JG002760>, 2015.

597 Tranvik, L. J. and Jansson, M.: Terrestrial export of organic carbon, *Nature*, 415, 861–862,  
598 <https://doi.org/10.1038/415861b>, 2002.

599 Viovy, N.: CRUNCEP Version 7 - Atmospheric Forcing Data for the Community Land Model,  
600 <https://doi.org/10.5065/PZ8F-F017>, 2018.

601 van Vliet, M. T. H., Yearsley, J. R., Franssen, W. H. P., Ludwig, F., Haddeland, I., Lettenmaier, D. P., and  
602 Kabat, P.: Coupled daily streamflow and water temperature modelling in large river basins, *Hydrology  
603 and Earth System Sciences*, 16, 4303–4321, <https://doi.org/10.5194/hess-16-4303-2012>, 2012.

604 Wang, Y., Xie, Z., Liu, S., Wang, L., Li, R., Chen, S., Jia, B., Qin, P., and Xie, J.: Effects of Anthropogenic  
605 Disturbances and Climate Change on Riverine Dissolved Inorganic Nitrogen Transport, *Journal of  
606 Advances in Modeling Earth Systems*, 12, e2020MS002234, <https://doi.org/10.1029/2020MS002234>,  
607 2020.

608 Wu, H., Peng, C., Moore, T. R., Hua, D., Li, C., Zhu, Q., Peichl, M., Arain, M. A., and Guo, Z.: Modeling  
609 dissolved organic carbon in temperate forest soils: TRIPLEX-DOC model development and validation,  
610 *Geosci. Model Dev.*, 7, 867–881, <https://doi.org/10.5194/gmd-7-867-2014>, 2014.

611 Xie, Z., Wang, L., Wang, Y., Liu, B., Li, R., Xie, J., Zeng, Y., Liu, S., Gao, J., Chen, S., Jia, B., and Qin,  
612 P.: Land Surface Model CAS-LSM: Model Description and Evaluation, *Journal of Advances in Modeling  
613 Earth Systems*, 12, e2020MS002339, <https://doi.org/10.1029/2020MS002339>, 2020.

614 Yao, Y., Tian, H., Pan, S., Najjar, R. G., Friedrichs, M. A. M., Bian, Z., Li, H., and Hofmann, E. E.:  
615 Riverine Carbon Cycling Over the Past Century in the Mid-Atlantic Region of the United States, *J  
616 Geophys Res Biogeosci*, 126, <https://doi.org/10.1029/2020JG005968>, 2021.

617 Yearsley, J.: A semi-Lagrangian water temperature model for advection-dominated river systems, *Water  
618 Resources Research - WATER RESOUR RES*, 45, <https://doi.org/10.1029/2008WR007629>, 2009.

619 Zeng, Y., Xie, Z., Yu, Y., Liu, S., Wang, L., Zou, J., Qin, P., and Jia, B.: Effects of anthropogenic water  
620 regulation and groundwater lateral flow on land processes, *Journal of Advances in Modeling Earth  
621 Systems*, 8, 1106–1131, <https://doi.org/10.1002/2016MS000646>, 2016.

622 Zeng, Y., Xie, Z., and Zou, J.: Hydrologic and Climatic Responses to Global Anthropogenic Groundwater  
623 Extraction, *Journal of Climate*, 30, 71–90, <https://doi.org/10.1175/JCLI-D-16-0209.1>, 2017.

624 Zhang, Y.: The review of the research of the riverine organic carbon cycle, *Journal of Henan Polytechnic  
625 University( Natural Science)*, 31, 344–351, <https://doi.org/10.16186/j.cnki.1673-9787.2012.03.006>,  
626 2012.

627 Zou, J., Xie, Z., Yu, Y., Zhan, C., and Sun, Q.: Climatic responses to anthropogenic groundwater  
628 exploitation: a case study of the Haihe River Basin, Northern China, *Clim Dyn*, 42, 2125–2145,  
629 <https://doi.org/10.1007/s00382-013-1995-2>, 2014.

630 Zou, J., Xie, Z., Zhan, C., Qin, P., Sun, Q., Jia, B., and Xia, J.: Effects of anthropogenic groundwater  
631 exploitation on land surface processes: A case study of the Haihe River Basin, northern China, *Journal*  
632 *of Hydrology*, 524, 625–641, <https://doi.org/10.1016/j.jhydrol.2015.03.026>, 2015.

633